Nonparabolicity of the conduction band and the coupled plasmon-phonon modes in n-GaAs

H. R. Chandrasekhar

Department of Physics, University of Missouri-Columbia, Columbia, Missouri 65211

A. K. Ramdas

Department of Physics, Purdue University, West Lafayette, Indiana 47907
(Received 1 October 1979)

We present the results of a detailed investigation of the infrared reflectivity spectra of n-GaAs as a function of doping such that the free-carrier plasma frequency is swept into and away from resonance with the LO-phonon frequency. The variation of the electron effective mass as a function of Fermi energy due to the nonparabolicity of the conduction band is accurately determined. Fits to the experimental data using $\vec{k} \cdot \vec{p}$ theory yield the value for the effective mass at the bottom of the conduction band, $m_0^* = (0.0665 \pm 0.0010)m_e$. The coupled plasmon-phonon modes are evaluated from the zeros of the real part of the total dielectric function with the variation of the effective mass versus doping included. At low carrier concentrations our data are in good agreement with the Raman scattering data of Mooradian *et al.*, but at high electron concentrations the contributions due to nonparabolicity of the conduction band are significant, as our data demonstrate.

I. INTRODUCTION

Yokota[1] and Varga[2] have shown that the long-wavelength plasmon of free carriers in a partially ionic semiconductor can interact with the infrared-active, zone-center optical phonons. More specifically, the interaction occurs with the longitudinal-optical phonons via the electric fields associated with both the phonons and the plasmon, the resulting coupled modes having both plasmon-like and LO-phonon-like characteristics.[2,3] The frequencies of the coupled modes are deduced from the "zeros" of the total dielectric function $\epsilon(\omega)$, it being assumed that the free-carrier and the lattice contributions are additive. Mooradian and Wright[4] gave the first experimental demonstration of these coupled modes; they reported the Raman lines associated with them in n-type gallium arsenide (n-GaAs). Mooradian and McWhorter[5] reported further observations on the polarization and intensity of the Raman lines. Such coupled modes can also manifest themselves in the infrared-reflectivity spectrum; from a curve fitting of the spectrum in terms of the plasma frequency ω_p and the LO-phonon frequency ω_l the coupled-mode frequencies can be determined. Following Olson and Lynch,[6] there have been several such studies in GaAs.[7-10]

It is well known that the effective mass (m^*) of electrons in the zone-center (Γ) conduction-band minimum of InSb, InAs, and GaAs varies as a function of carrier concentration, a consequence of the nonparabolicity of the conduction band.[11] Since m^* determines ω_p, the effects of nonparabolicity on the coupled-mode frequencies are clear-ly of interest. A variety of experimental techniques[12] give m^*/m_e at the bottom of the Γ minimum of GaAs close to 0.0648 ± 0.0015 as determined by Chamberlain and Stradling[13] from cyclotron resonance. In contrast, Spitzer and Whelan[14] obtained $m^*/m_e = 0.086$ from plasma-edge measurements on a sample having a carrier concentration of 5.4×10^{18} cm^{-3}. Olson and Lynch[6] were able to obtain evidence for the variation of m^*/m_e in their study of the coupled modes in n-GaAs from the infrared-reflectivity spectrum; they saw an increase from 0.067 to 0.077 as the carrier concentration was increased from 7.22×10^{17} to 1.4×10^{18} cm^{-3}. Mooradian and co-workers[4,5] however analyzed their data on the coupled modes in the Raman effect for samples covering a concentration range 2.3×10^{15} to 2.9×10^{18} cm^{-3} in terms of $m^*/m_e = 0.07$. We have remeasured the infrared-reflectivity spectra of n-GaAs with carrier concentration ranging from 1.8×10^{16} to 7×10^{18} cm^{-3} and have obtained high-quality spectra covering a wide spectral range. The free-carrier plasmon frequency (ω_p) is thus swept into and away from resonance with the LO-phonon frequency (ω_l). In this paper we report these measurements and show that their analysis requires that a proper allowance be made for the nonparabolicity of the Γ minimum. We also compare our data with those obtained in earlier Raman and infrared studies.

II. THEORY

The interaction of long-wavelength longitudinal-vibrational modes with the longitudinal-collective

excitations of plasmons becomes significant when ω_p approaches ω_l where

$$\omega_p = \left(\frac{4\pi N e^2}{m^* \epsilon_\infty}\right)^{1/2}. \tag{1}$$

Here N is the free-carrier concentration, m^* the effective mass of the carrier, and ϵ_∞ the optical dielectric constant. In the long-wavelength limit, the total dielectric constant can be written as the sum of the lattice and free-carrier contributions, i.e.,

$$\epsilon(\omega) = \epsilon_1(\omega) + i\epsilon_2(\omega)$$
$$= \epsilon_\infty + \frac{\epsilon_0 - \epsilon_\infty}{1 - (\omega/\omega_t)^2 - i\gamma(\omega/\omega_t^2)} - \frac{\epsilon_\infty \omega_p^2}{\omega(\omega + i\gamma_p)}, \tag{2}$$

where ω_t is frequency of the transverse-optic (TO) phonons. The phonon and plasmon damping parameters γ and γ_p, respectively, are frequency-dependent in general and the Lydanne-Sachs-Teller relation relates ω_t, ω_l, ϵ_0, and ϵ_∞. At normal incidence, reflectivity is related to $\epsilon(\omega)$ via the index of refraction n and the extinction coefficient k by

$$R = \frac{(n-1)^2 + k^2}{(n+1)^2 + k^2}, \tag{3}$$

$$n^2 - k^2 = \epsilon_1(\omega), \tag{4}$$

and

$$2nk = \epsilon_2(\omega). \tag{5}$$

The reflectivity spectra exhibit two sharp dips in the absence of damping. The frequencies of two minima in the limit of zero damping can be evaluated from Eq. (3) to be

$$\omega_{min}^2 = \frac{[\epsilon_0(1 + \omega_p^2/\omega_t^2) - 1] \pm \{[\epsilon_0(1 + \omega_p^2/\omega_t^2) - 1]^2 - 4\epsilon_0(\epsilon_\infty - 1)\omega_p^2/\omega_t^2\}^{1/2}}{2(\epsilon_\infty - 1)/\omega_t^2}. \tag{6}$$

The frequencies of coupled plasmon-phonon modes defined as the solutions of $\epsilon_1(\omega) = 0$ are given by

$$\omega_{\pm}^2 = \frac{\omega_t^2 + \omega_p^2}{2} \pm \left[\left(\frac{\omega_t^2 + \omega_p^2}{2}\right)^2 - \omega_p^2 \omega_t^2\right]^{1/2}. \tag{7}$$

However, as the damping coefficients increase, Eqs. (6) and (7) are no longer valid. The two sharp dips in the reflectivity minima get smeared out and the coupled-mode frequencies become complex. This is indeed the case for p-GaAs which exhibits γ_p about a factor of 10 larger than that for n-GaAs.[15]

Analysis of the reflectivity spectra of a doped polar semiconductor can be used to determine various optical constants as a function of carrier concentration from the above equations. If the carrier concentration is known independently, the effective mass m^* can be determined from Eq. (1). In the case of an isotropic parabolic band, the optically determined effective mass m^*_{opt} is identical to m^*. However, this is not the case for a nonparabolic band which results in a variation of the effective mass with carrier concentration given by[11,16] the $\vec{k} \cdot \vec{p}$ theory as

$$\frac{1}{m^*_{opt}} = \frac{1}{m_0^*}\left[1 - \frac{10 k_B T}{3 E_g}\left(\frac{F_{3/2}}{F_{1/2}}\right)\right]. \tag{8}$$

Here m_0^* is the effective mass at the bottom of the conduction band, E_g the energy gap at temperature T, and $F_{3/2}$ and $F_{1/2}$ are the Fermi integrals.[17] The values of the Fermi integrals at a given temperature and carrier concentration N can be determined from

$$N = \frac{\sqrt{2}(k_B T)^{3/2} m_0^{*3/2}}{\pi^2 \hbar^3}\left(F_{1/2} + \frac{5 k_B T}{2 E_g} F_{3/2}\right). \tag{9}$$

III. EXPERIMENT AND ANALYSIS OF DATA

High quality single crystals of tellurium doped GaAs were polished and etched with an aqueous solution of NaOCl immediately prior to the measurement. During the measurements the samples were maintained in vacuum or dry air. Good surface quality was essential to obtain reproducible reflectivity data within 2%. The spectra were re-
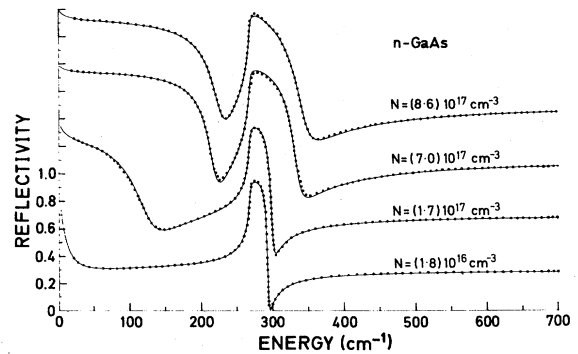

FIG. 1. Experimental (solid points) and theoretical (solid lines) reflectivity spectra of n-GaAs for carrier concentrations 1.8×10^{16}, 1.7×10^{17}, 7.0×10^{17}, and 8.6×10^{17} cm^{-3}. The reflectivity scale refers to the sample with the concentration 1.8×10^{16} cm^{-3}. The reflectivity spectra for the other samples have been vertically shifted for clarity by 0.4 for successively higher concentration.
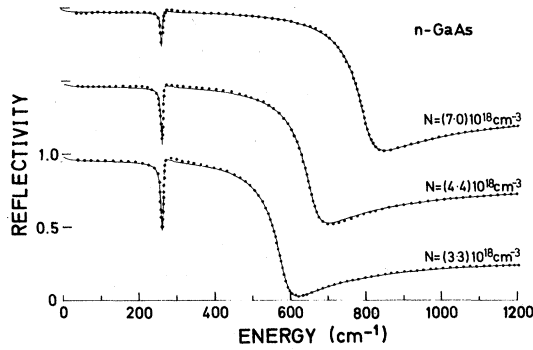
FIG. 2. Experimental (solid points) and theoretical (solid lines) reflectivity spectra of n-GaAs for carrier concentrations 3.3×10^{18}, 4.4×10^{18}, and 7.0×10^{18} cm^{-3}. The reflectivity scale refers to the sample with the concentration 3.3×10^{18} cm^{-3}. For the others, they are vertically shifted for clarity by 0.5 for successively higher concentration.

corded using a Polytec FIR30 Fourier spectro-meter[18] in the 10–450 cm^{-1} range and a Perkin-Elmer (Model 180) grating spectrophotometer[19] in the 200–4000 cm^{-1} range. Hall coefficient mea-surements were performed on different parts of the ingot from which the samples for reflectivity measurements were obtained. Accurate values of the carrier concentration and mobility were hence determined. The measured reflectivity spectra were digitized. A least-squares minimization al-gorithm[20] to fit the data to the theoretical expres-sions of Eqs. (2)–(5) was used. The solid curves in Figs. 1 and 2 are such fits to the experimental data (solid points). Factorized forms of the di-electric function[10,21] were also used to improve the fits and found to be unnecessary. The Eqs. (2)–(5) adequately describe the reflectivity spec-tra of n-GaAs. However, in the case of several closely spaced oscillators,[21] multicomponent plas-mons,[15] and large damping,[15,22] more complicated forms of the dielectric function are necessary to fit the data.

IV. DISCUSSION

Table I lists the best-fit parameters from the fits to the experimental data of Figs. 1 and 2 using Eqs. (2)–(5). The coupled-mode frequencies shown are from Eq. (7). There is no shift in the transverse-optic phonon mode as a function of car-rier concentration within experimental error. This was confirmed by keeping ω_t and ω_l fixed at the value for pure GaAs; the fits thus obtained yielded the same values for the other parameters. In Fig. 3 we show a plot of the effective mass determined from Eq. (1) and the plasma frequency (ω_p) vs the carrier concentration. Also shown for comparison are the results of the Faraday rotation measurements of Piller.[23] The solid curves 1, 2, and 3 are from the theoretical expressions of Eqs. (8) and (9) and the values of the effective mass at the bottom of the conduction band $m_0^*/m_e = 0.065$, 0.066, and 0.067. There is a noticeable scatter in the data for low carrier concentrations. How-ever, at high carrier concentrations curves 2 and 3 fit the data well. From this analysis the value of m_0^*/m_e is determined to be 0.0665 ± 0.0010 at room temperature. This value is in good agree-ment with that obtained from various methods (see Table II of Ref. 12).

Figure 4 shows a plot of ω_p, ω_+, and ω_- as a function of the square root of the carrier concen-tration. We have included the Raman scattering results of Mooradian et al.[5] for comparison. These authors however did not consider the effects of nonparabolicity but used a constant value for $m^* = (0.067)m_e$; on that assumption the plot of ω_p vs $N^{1/2}$ would be a straight line as shown by the dashed line in Fig. 4. This agrees reasonably well with the experimental data (open circles) for low carrier concentrations. However, at large carrier concentrations the discrepancy becomes noticeable. A good fit to the data can be obtained by including a carrier concentration dependent m_{opt}^* given by Eqs. (8) and (9). The solid theoreti-cal curves for ω_+ and ω_- fit both the infrared and Raman data well. The assumption of an additive

TABLE I. The frequencies of plasmon and phonon modes, the coupled modes and the damping coefficients obtained from the fits to the experimental data on reflectivity as a function of frequency.

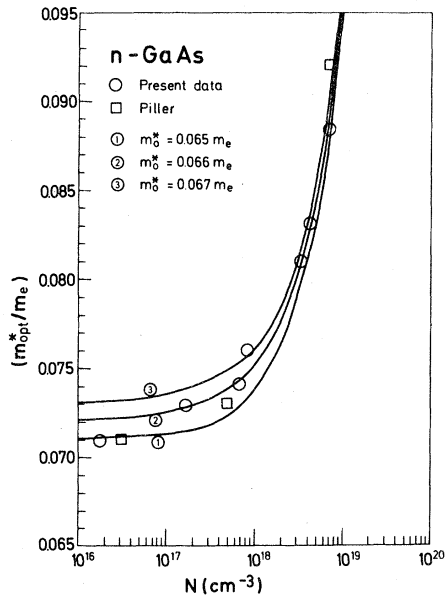| N (10^{16} cm^{-3})	ω_t (cm^{-1})	ω_l (cm^{-1})	γ (cm^{-1})	ω_p (cm^{-1})	γ_p (cm^{-1})	ω_+ (cm^{-1})	ω_- (cm^{-1})
1.8	268.0	292.0	1.85	45	50	293	41.2
17	267.5	290.5	2.7	136	62	298	122.3
70	267.8	290.1	2.4	275	47	336	219.6
86	268.3	294.0	1.8	300	62	350	230
330	267.4	291.5	2.5	570	61	585	261
440	267.7	292.5	2.9	650	55	662	263
700	267.0	291.3	2.9	795	69	805	265

FIG. 3. Electron effective mass versus carrier concentration obtained from the present experimental data using Eq. (1) (open circles) and the results on Faraday rotation measurements by Piller (Ref. 23) (open squares). The solid curves are theoretical fits to the data using Eqs. (8) and (9) with m_0^*/m_e, characterizing the bottom of the Γ minimum = 0.065, 0.066, and 0.067 for curves 1, 2, and 3, respectively.

FIG. 4. The longitudinal optical (ω_l) and the transverse optical (ω_t) phonon frequencies, plasma frequency (ω_p), and the coupled plasmon-phonon mode frequencies ($\omega_{\pm}$) of n-GaAs as a function of the square root of the carrier concentration (N). The open triangles and circles are from the fits to the present data and the open squares are from the Raman scattering data of Mooradian and McWhorter (Ref. 5). The dashed line represents ω_p vs $N^{1/2}$ using Eq. (1) with $m_0^*/m_e = 0.066$. The solid line representing ω_p vs $N^{1/2}$ includes the variation of m^* with carrier concentration. The solid curves for $\omega_{\pm}$ are computed from Eq. (7).

plasmon-phonon dielectric function adequately describes the data for n-GaAs. As shown in Table I, γ and γ_p are substantially small compared to ω_t and Eq. (7) is valid.

The effect of temperature on the effective mass has been described by several authors.[24,25] The nonparabolicity of the bands tends to increase m_{opt}^* with increasing temperature as the electrons are excited to higher energies. However, the corresponding decrease in the band gap tends to decrease m^* and, in turn m_{opt}^*, with increasing temperature. The net effect would thus be very small. The decrease in m^* has been estimated[24] to be 2.5% as the temperature is raised from 100 to 300 K. This is in excellent agreement with the magneto-phonon measurements of Stradling and Wood.[26] We performed the infrared-reflectivity measurements on a sample with carrier concentration 7×10^{18} cm^{-3} for different temperatures

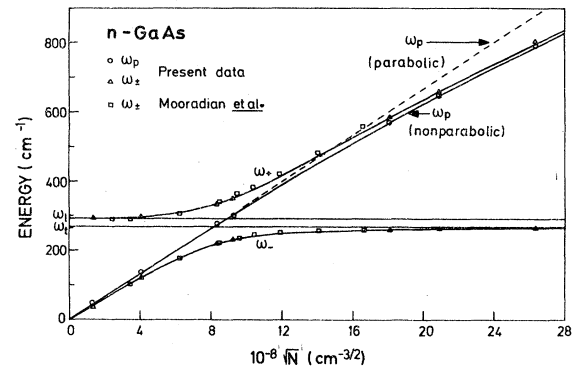and found an increase in the effective mass of ~2% between 78 and 296 °K which agrees well with the theory.

[1]I. Yokota, J. Phys. Soc. Jpn. 16, 2075 (1961).
[2]B. B. Varga, Phys. Rev. 137, A1896 (1965).
[3]K. S. Singwi and M. P. Tosi, Phys. Rev. 147, 658 (1966).
[4]A. Mooradian and G. B. Wright, Phys. Rev. Lett. 16,

999 (1966).
[5]A. Mooradian and A. L. McWhorter, Phys. Rev. Lett. 19, 849 (1967); A. Mooradian and A. L. McWhorter, in Light Scattering Spectra of Solids, edited by G. B. Wright (Springer, New York, 1969), p. 297.

[6]C. G. Olson and D. W. Lynch, Phys. Rev. 177, 1231 (1963).

[7]S. Perkowitz and J. Breecher, Infrared Phys. 13, 321 (1973).

[8]R. T. Holm, J. W. Gibson, and E. D. Palik, J. Appl. Phys. 48, 212 (1977). In this investigation, the authors focus their attention on reflectivity data as a means of characterizing the material in terms of its carrier concentration and the mobility of the carriers assuming $m*/m_e$ from other measurements.

[9]N. K. S. Gaur, Physica 64, 613 (1973).

[10]A. A. Kukarskii, Solid State Commun. 13, 1761 (1973).

[11]For a review, see O. Madelung, *Physics of III-V Compounds* (Wiley, New York, 1964).

[12]G. E. Stillman, C. M. Wolfe, and J. O. Dimmock, in *Semiconductors and Semimetals*, edited by R. K. Willardson and A. C. Beer (Academic, New York, 1977), Vol. 12, p. 169. See, in particular, Table II, p. 182.

[13]J. M. Chamberlain and R. A. Stradling, Solid State Commun. 7, 1275 (1969).

[14]W. G. Spitzer and J. M. Whelan, Phys. Rev. 114, 59 (1959).

[15]D. Olego, H. R. Chandrasekhar, and M. Cardona, in *Physics of Semiconductors 1978*, edited by B. L. H. Wilson (The Institute of Physics, Bristol, 1979),

p. 1313.

[16]E. O. Kane, J. Phys. Chem. Solids 1, 249 (1957).

[17]See for example, O. Madelung, in *Encyclopedia of Physics*, edited by S. Flügge (Springer, Berlin, 1957), Vol. 20, p. 1.

[18]Polytec, 7501 Wettersbach-Karlsruhe, West Germany.

[19]Perkin-Elmer Corporation, Norwalk, Connecticut.

[20]A modified Levenberg-Marquardt algorithm was used. See, for example, K. M.Brown and J. E. Dennis, Numerische Mathematik 18, 289 (1972).

[21]See for example, H. R. Chandrasekhar, G. Burns, and G. V. Chandrasekhar, Solid State Commun. 27, 829 (1978).

[22]F. Gervais and J. F. Baumard, Solid State Commun. 21, 861 (1977); J. L. Servoin and F. Gervais, Appl. Opt. 16, 2952 (1977).

[23]H. Piller, J. Phys. Soc. Jpn. 21, Suppl. 206 (1966).

[24]M. Cardona, Phys. Rev. 121, 752 (1961).

[25]W. M. DeMeis, Ph.D. thesis, Harvard University and Technical Report No. HP-15, Gordon McKay Laboratory, Division of Engineering and Applied Physics, Harvard University, 1965.

[26]R. A. Stradling and R. A. Wood, J. Phys. C 1, 1711 (1968).